The Response of Prostate Smooth Muscle Cells to Testosterone Is Determined by the Subcellular Distribution of the Androgen Receptor

Nahuel Peinetti,[1,2] María Victoria Scalerandi,[1,2] Mariana Micaela Cuello Rubio,[1,2] Carolina Leimgruber,[1,2] Juan Pablo Nicola,[3,4] Alicia Ines Torres,[1,2] Amado Alfredo Quintar,[1,2]* and Cristina Alicia Maldonado[1,2]*

[1]Universidad Nacional de Córdoba, Facultad de Ciencias Médicas, Centro de Microscopía Electrónica. 5000 Córdoba, Argentina; [2]Consejo Nacional de Investigaciones Científicas y Técnicas, Instituto de Investigaciones en Ciencias de la Salud (INICSA), 5000 Córdoba, Argentina; [3]Universidad Nacional de Córdoba, Facultad de Ciencias Químicas, Departamento de Bioquímica Clínica, 5000 Córdoba, Argentina; and [4]Consejo Nacional de Investigaciones Científicas y Técnicas, Centro de Investigaciones en Bioquímica Clínica e Inmunología, 5000 Córdoba, Argentina

Androgen signaling in prostate smooth muscle cells (pSMCs) is critical for the maintenance of prostate homeostasis, the alterations of which are a central aspect in the development of pathological conditions. Testosterone can act through the classic androgen receptor (AR) in the cytoplasm, eliciting genomic signaling, or through different types of receptors located at the plasma membrane for nongenomic signaling. We aimed to find evidence of nongenomic testosterone-signaling mechanisms in pSMCs and their participation in cell proliferation, differentiation, and the modulation of the response to lipopolysaccharide. We demonstrated that pSMCs can respond to testosterone by a rapid activation of ERK1/2 and Akt. Furthermore, a pool of ARs localized at the cell surface of pSMCs is responsible for a nongenomic testosterone-induced increase in cell proliferation. Through membrane receptor stimulation, testosterone favors a muscle phenotype, indicated by an increase in smooth muscle markers. We also showed that the anti-inflammatory effects of testosterone, capable of attenuating lipopolysaccharide-induced proinflammatory actions, are promoted only by receptors located inside the cell. We postulate that testosterone might perform pro-homeostatic effects through intracellular-initiated mechanisms by modulating cell proliferation and inflammation, whereas some pathological, hyperproliferative actions would be induced by membrane-initiated nongenomic signaling in pSMCs. (***Endocrinology*** **159: 945–956, 2018)**

Prostate smooth muscle cells (pSMCs) are stromal cells of the prostate gland that, along with fibroblasts, form the layer underlying the epithelial compartment (1). Under normal conditions, these cells are involved in the preservation of organ homeostasis by regulating the adjacent epithelial cells through androgen-dependent paracrine signaling (2). However, alterations in the microenvironment can induce changes in the pSMC phenotype that can affect stromal-epithelial interactions. We previously demonstrated that pSMCs dedifferentiate in response to lipopolysaccharide (LPS) to acquire a myofibroblast-like secretory profile, contributing to prostatic inflammation *in vivo* and *in vitro* (3, 4). Furthermore, pSMCs lose their normal phenotype in response to hormonal imbalance and inflammation during benign prostatic hyperplasia (BPH) (5, 6) and prostate cancer (7).

Androgens, especially testosterone and its metabolite, dihydrotestosterone, are vital for prostate development and function (8). pSMCs from rat ventral prostate express high levels of classic androgen receptors (ARs) (9), and it has been demonstrated that cell morphology (10),

ISSN Online 1945-7170

Received 6 August 2017. Accepted 22 November 2017.
First Published Online 29 November 2017

*These authors contributed equally to this study.

Abbreviations: AR, androgen receptor; ARE, androgen response element; BPH, benign prostatic hyperplasia; BSA, bovine serum albumin; cDNA, complementary DNA; FBS, fetal bovine serum; LPS, lipopolysaccharide; mAR, membrane androgen receptor; NF-κB, nuclear factor κB; PBS, phosphate-buffered saline; pSMC, prostate smooth muscle cell; qPCR, quantitative polymerase chain reaction; TGFβ1, tumor growth factor β1.

as well as smooth muscle phenotype, are highly influenced by circulating levels of testosterone (11). We have reported an increase in the expression of smooth muscle markers in correlation with testosterone concentration in normal and inflammation-induced dedifferentiated cells *in vitro* (12, 13). Previous reports have also indicated that testosterone is capable of increasing prostate stromal cell proliferation (13, 14), confirming the importance of androgens as regulators of the cell cycle. Indeed, androgen blockade is of particular medical interest for the treatment of hyperproliferative conditions such as BPH or prostate cancer. Conversely, we have shown that testosterone prevents and reverts inflammation-induced proliferation by dampening the inflammatory scenario, leading to a decrease in nuclear factor κB (NF-κB) nuclear translocation and, consequently, cytokine secretion (12, 13). The mechanisms that may help explain these differential androgen effects on cell proliferation and inflammatory response have not been elucidated.

Classic androgen signaling is activated when testosterone is recognized by the cytosolic AR and the complex migrates to the nucleus to bind androgen response elements (AREs) in the DNA (15). However, according to accumulated evidence, androgens and other steroid hormones can also signal through nonclassic (or nongenomic) mechanisms (16). Different types of receptors, including AR (17, 18), GPCR (19), and ZIP9 (20), induce nongenomic signaling, which produces a rapid activation of transduction pathways (18). Of note, prostate epithelial cells (21–23) and uncharacterized cells from the stromal compartment (24) respond to nongenomic androgen actions. Many of these nongenomic pathways are triggered by a population of ARs, which, likely after palmitoylation in the cytosol, translocate to the plasma membrane (25), behaving as strong activators of proliferation in prostate epithelial cells (26–29), skeletal muscle myoblasts (30), and breast cancer cells (25). Strikingly, signaling through other membrane receptors for testosterone inhibits cell proliferation in the prostatic cancer epithelial cell line LNCaP (31).

Considering the diverse effects triggered by testosterone, we hypothesized that more than one signaling pathway may be activated by this hormone on pSMCs. Our aim, therefore, was to determine the presence and functionality of membrane androgen receptors (mARs) and nongenomic androgen signaling in pSMCs.

Materials and Methods

Animals

Adult Wistar male rats (12 weeks old), weighing 250 to 350 g, were housed at the Animal Research Facility of the National University of Córdoba, Córdoba, Argentina, in air-conditioned quarters and under a controlled photoperiod (14 hours of light, 10 hours of darkness) with free access to commercial rodent food and tap water. Animal care and procedures were conducted following the recommendations of the guidelines of National Institutes of Health for the care of and use of laboratory animals. All animal experiments were approved by the committee for the care and use of experimental animals of the School of Medicine, National University of Córdoba.

Cell cultures and treatments

Prostate glands were obtained from six Wistar rats per culture. Cell culture protocols have been described previously (4). Briefly, tissues were minced and treated for 30 minutes with a digestion solution containing 200 U/mL collagenase type IA (Sigma-Aldrich, St. Louis, MO) in MCDB131 medium (Sigma-Aldrich). Dispersed cells were seeded on six-well culture plates and cultured in MCDB131 supplemented with 15% heat-inactivated fetal bovine serum (FBS; Internegocios, Buenos Aires, Argentina) in a humidified incubator at 37°C in a 5% CO_2 atmosphere. The culture medium was replaced every 2 days until confluence, after which cells were detached and reseeded in double the number of plates. To differentiate stromal cells into pSMCs, the medium was replaced by serum-free MCDB131 supplemented with 5 mg/mL insulin, 5 mg/mL transferrin, 5 ng/mL selenite, and 2 ng/mL tumor growth factor β1 (TGFβ1; Invitrogen, Waltham, MA) for 72 hours with replacement every 24 hours. After that, pSMCs were treated with the following stimuli: testosterone (10^{-7} M); membrane-impermeable testosterone-3-(*O*-carboxymethyl)oxime and bovine serum albumin (BSA) conjugate (testosterone-BSA; Sigma-Aldrich); or its vehicles for 24 or 48 hours. Before each experiment, a new solution of testosterone-BSA was prepared and subjected to treatment with 0.05 mg/mL dextran and 50 mg/mL charcoal for 30 minutes to remove any potential contamination with free testosterone, and later was centrifuged at 3000*g* for 10 minutes and filtered through 0.22-μm filters (Merck Millipore, Billerica, MA) (31). For immunomodulation studies, the cells were stimulated with 1 μg/mL LPS, LPS with testosterone, or LPS with testosterone-BSA for 24 to 72 hours. For inhibitor assays, we used 10^{-5} M U0126 (Sigma-Aldrich), 10^{-7} M hydroxyflutamide (Sigma-Aldrich), or 10^{-8} M 2-bromopalmitate for 20 minutes before stimulation.

LnCap and PC3 cell lines were provided by Dr. Chang from the University of Rochester, Rochester, New York, and maintained in Roswell Park Memorial Institute 1640 medium supplemented with 10% FBS. Cells were stimulated with LPS 10 μg/mL for 6 hours or TNFα 5ng/mL for 24 hours and subjected to RNA extraction and quantitative polymerase chain reaction (qPCR) analysis.

Immunofluorescence

After stimuli, pSMCs were washed with phosphate-buffered saline (PBS) and fixed with 4% formaldehyde. Cell permeabilization was performed using 0.25% triton X-100 and blocked with PBS containing 5% BSA for 30 minutes. Cells were incubated overnight in a humidified chamber with the primary antibodies listed in Table 1. Afterward, cells were washed three times with PBS and incubated with Alexa 594 anti-mouse or Alexa 594 anti-rabbit antibody for 1 hour at room temperature. Incubation with 4′,6-diamidino-2-phenylindole was used to stain cell nuclei, and coverslips were mounted using fluoromount (Sigma-Aldrich). To validate the specificity of the

Table 1. Antibody Table

Antibody Name	Technique (Concentration)	Target Antigen	Manufacturer, Catalog No.	Species Raised in; Monoclonal or Polyclonal	RRID	Reference
Mouse Anti-Human α–Smooth Muscle Actin Monoclonal Antibody	ICC (1:100); WB (1:200)	α–Smooth muscle actin human, mouse, rat	Leica Microsystems, NCL-SMA	Mouse; monoclonal	AB_442134	PMID: 3312298
Anti-Vimentin Monoclonal Antibody	ICC (1:100); WB (1:300)	Vimentin human	Leica Microsystems, NCL-L-VIM-V9	Mouse; monoclonal	AB_564055	PMID: 2447807
Calponin 1 Monoclonal Antibody (CALP)	ICC (1:500); WB (1:500)	Calponin 1 human	Thermo Fisher Scientific, MA5-11620	Mouse; monoclonal	AB_10983410	PMID: 16140947
NF-κB p65 antibody - ChIP Grade	ICC (1:1000); WB (1:1000) FC (1:1000)	NF-κB p65 - ChIP grade human, mouse, rat	Abcam, ab7970	Rabbit; polyclonal	AB_306184	
Androgen Receptor antibody - ChIP grade	FC (1:200)	N-terminus of the rat androgen receptor	Millipore, 06-680	Rabbit; polyclonal	AB_310214	
Androgen Receptor antibody	ICC (1:200); WB (1:1000)	Androgen receptor antibody - ChIP grade human, mouse, rat	Abcam, ab74272	Rabbit; polyclonal	AB_1280747	PMID: 28609657
Ki-67 antibody	ICC	Ki-67 human	BD Biosciences, 550609	Mouse; monoclonal	AB_393778	PMID: 7520455
ERK 1 (K-23) antibody	WB (1:500)	ERK 1 (K-23) mouse, rat, hamster, mouse, rat, human, chicken, frog, human	Santa Cruz Biotechnology, sc-94	Mouse; monoclonal	AB_2140110	PMID: 19326470
ERK1/2	WB (1:200)	ERK 1/2 antibody	Santa Cruz Biotechnology, sc-292838	Rabbit; polyclonal	AB_2650548	
Phospho-p44/42 MAPK (Erk1/2) (Thr202/Tyr204) (197G2) Rabbit mAb	WB (1:1000)	Goat rabbit IgG (H+L)-HRP conjugate	Cell Signaling Technology, 4377S	Rabbit; polyclonal	AB_331775	PMID: 24422540
Akt	WB (1:300)	Amino acids 71–184 of Akt1 of human origin	Santa Cruz Biotechnology, sc-125829	Mouse; monoclonal	AB_2224733	
Phospho-Akt (Ser473) antibody	WB (1:200)	Ser473	Cell Signaling Technology, 4060S	Rabbit; monoclonal	AB_2315049	PMID: 23749404
Rabbit anti-Mouse IgG (H+L) Cross-Adsorbed Secondary Antibody, Alexa Fluor 594	ICC (1:1000)	Mouse IgG (H+L) cross-adsorbed mouse	Thermo Fisher Scientific, A-11062	Rabbit; polyclonal	AB_2534109	PMID: 28575672
Goat Anti-Rabbit IgG (H+L) secondary antibody, Alexa Fluor 647 conjugate	FC (1:1000)	γ-Immunoglobulins, H+L	Thermo Fisher Scientific, A-21244	Goat; polyclonal	AB_2535812	
Goat Anti-Mouse IgG (H+L) Secondary Antibody, Alexa Fluor 488 conjugate	FC (1:1000)	γ-Immunoglobulins, H+L	Thermo Fisher Scientific, A-11001	Goat; polyclonal	AB_2534069	
Donkey anti-rabbit IgG (H+L) Secondary Antibody, Alexa Fluor® 594 conjugate	ICC (1:1000) FC	Rabbit IgG (H+L) rabbit	Thermo Fisher Scientific, A21207	Donkey; polyclonal	AB_141637	PMID: 24302627
Anti-Mouse Ig (Whole Ab) Antibody, Biotin Conjugated	ICC (1:100)	Mouse Ig (whole Ab) mouse	GE Healthcare, RPN1001-2ML	Sheep; polyclonal	AB_1062579	
Peroxidase-AffiniPure goat anti-mouse IgG (H+L) (min × Hu,Bov,Hrs, Rb,Sw Sr Prot) antibody	WB (1:2500)	Mouse IgG (H+L) mouse	Jackson Immuno Research Labs, 115-035-146	Goat; polyclonal	AB_2307392	PMID: 25474204
Goat anti-rabbit IgG (H L)-HRP Conjugate antibody	WB (1:5000)	Goat rabbit IgG (H+L)–HRP conjugate	Bio-Rad, 170-6515	Goat; polyclonal	AB_11125142	PMID: 23515285

Abbreviations: Ab, antibody; ChIP, chromatin immunoprecipitation; ERK, extracellular signal-regulated kinase; FC, flow cytometry; H+L, heavy and light chains; HRP, horseradish peroxidase; ICC, immunocytochemistry; Ig, immunoglobulin; IgG, immunoglobulin G; mAb, monoclonal antibody; MAPK, mitogen-activated protein kinase; PMID, PubMed Identifier; RRID, Research Resource Identifier; WB, Western blot.

immunostaining, controls were performed by applying the same protocol but replacing the primary antibody with PBS containing 1% BSA.

For mAR staining, nonpermeabilized live cells were incubated with anti-AR overnight at 4°C before fixation. To control the integrity of the plasma membrane during the protocol, anti-AR antibody was replaced by anti-p65 NF-κB (intracellular protein). Concanavalin A-fluorescein isothiocyanate (1:30 dilution; Sigma-Aldrich), a lectin that specifically binds to the α-mannosyl saccharides expressed in the core structures of membrane glycoproteins, was used as a membrane marker. Images were then obtained using epifluorescent Axioplan microscopy (Zeiss, Oberkochen, Germany) or a confocal laser scanning microscope (FluoView FV 1200; Olympus; Tokyo, Japan). Images were processed using the FV10-ASW 1.6 viewer or Image J (National Institutes of Health, Bethesda, MD) software. To determine the number of mAR-positive cells, a total of 3000 pSMCs were counted from three independent cultures.

Analysis of cell surface proteins by cell surface biotinylation

The cell surface proteins were isolated using the Pierce cell surface protein isolation kit (Thermo Fisher Scientific, Waltham, MA) according to manufacturer´s instructions. Briefly, pSMCs from eight six-well plates were washed three times with ice-cold PBS buffer and then incubated with the membrane-impermeable sulfo-NHS-biotin at 4°C for 20 minutes. After biotinylation, the cultures were washed three times with ice-cold PBS and harvested with lysis buffer containing 1.25% Igepal CA-630, 2 mM phenylmethylsulfonyl fluoride, 10 μg/mL leupeptin, and 10 μg/mL aprotinin (all from Sigma-Aldrich). The cellular extracts were sonicated and incubated with avidin-agarose beads for 2 hours at 4°C. Then, the extracts were centrifuged at 500*g* for 10 minutes at 4°C, the supernatant was separated, and the pellet was washed three times with 1 mL of lysis buffer. The pellets from the eight culture plates were concentrated and seeded in a single lane of a 12% acrylamide gel. The surface protein fraction and the total homogenate were analyzed by western blot using rabbit anti-AR. The cytosolic/nuclear protein p65 was used as a control for purity of the surface-protein fraction.

Flow cytometry

Cells from each culture were divided into two groups for detection of either intracellular AR or mAR. For intracellular AR, cells were detached by TrypLE Express (Invitrogen) and fixed (Cytofix; BD Biosciences Pharmingen, San Diego, CA) for 20 minutes at 4°C, permeabilized with Perm/Wash buffer (BD Biosciences), and incubated with anti-AR overnight at 4°C. pSMCs were washed with Perm/Wash buffer followed by incubation with secondary antibody conjugated to Alexa 647 for 1 hour at room temperature. Cells were washed, suspended in filtered PBS, and analyzed by Cytoron absolute flow cytometer (Ortho Diagnostic System, Raritan, NJ). For mAR detection, after being detached from the culture plate, live cells were washed with PBS containing 2% FBS and incubated overnight at 4°C with anti-AR antibody. After washing, cells were incubated with secondary antibody for 1 hour at 37°C and consequently treated with Cytofix for 20 minutes, dispersed in PBS, and analyzed by flow cytometry. Analysis was done with Flowjob software (Tree Star, Ashland, OR). As negative control, cells were incubated with immunoglobulin G isotype instead of the primary antibody. To control the integrity of the plasma membrane during the protocol, primary antibody for intracellular protein p65 was used instead of anti-AR.

Western blot

Cell were washed with ice-cold PBS and lysed with 120 μL of lysis buffer (1.25% Igepal CA-630, 1 mM EDTA, 2 mM phenylmethylsulfonyl fluoride, 10 μg/mL leupeptin, and 10 μg/mL aprotinin, 40 μg/mL sodium fluoride, 100 μg/mL sodium pyrophosphate, and PBS) per well. The lysate was centrifuged at 14,000*g* for 20 minutes at 4°C to pellet the Igepal CA-630–insoluble material. Samples were incubated with loading buffer (Tris buffer containing 0.5% glycerol, 0.1% sodium dodecyl sulfate, 10% 2-mercaptoethanol, 0.002% bromophenol blue) and heated at 95°C for 5 minutes. Proteins were separated on 12% sodium dodecyl sulfate–polyacrylamide gels and blotted onto a Hybond-C membrane (Amersham Pharmacia, Buckinghamshire, UK). Membranes were blocked for 30 minutes with Tris-buffered saline containing 0.1% Tween 20, 5% BSA. Membranes were incubated overnight with primary antibodies (Table 1) diluted in PBS containing 0.1% Tween 20, 1% BSA, and afterward were washed three times with PBS containing 0.1% Tween 20. Membranes were incubated with anti-mouse or anti-rabbit secondary antibodies conjugated to horseradish peroxidase diluted in Tris-buffered saline containing 0.1% Tween 20, 1% BSA, and revealed with an enhanced chemiluminescence detection system (ECL; Amersham Biosciences, Buckinghamshire, UK). Emitted light was captured on hyperfilm (Amersham Pharmacia) or the C-Digit blot scanner (Li-Cor, Lincoln, NE), following the manufacturer's instructions. The densitometry analyses were performed by applying the Image J software (National Institutes of Health, Bethesda, MD). The relative expression was calculated via comparison with the loading control and different treatments were relativized to the control group (100%).

Proliferation assay

pSMCs grown on coverslips were stimulated with testosterone or testosterone-BSA in the presence or absence of inhibitors hydroxyflutamide or U0126 for 24 hours. Cells were fixed with 4% formaldehyde and permeabilized with 0.5% Triton X-100 for 10 minutes. Nonspecific immunoreactivity was blocked with PBS containing 5% BSA for 30 minutes at room temperature, and the cells were incubated overnight with a monoclonal antibody against Ki67 at 4°C in a wet chamber. After washing with PBS, cells were incubated with a biotinylated anti-mouse secondary antibody. The coverslips were washed again with PBS, and the pSMCs were incubated with the avidin–biotin peroxidase complex (ABC; Vector, Burlingame, CA) for 30 minutes at room temperature. The immunoreactivity for Ki67 was visualized with 3,3-diaminobenzidine tetrahydrochloride as chromogen. A total of 1,000 cells were examined by light microscopy in randomly chosen fields of each glass slide to establish the percentage of Ki67 immunoreactive cells. Three slides were analyzed for each group, derived from the same cell preparations.

To count the total cell number, we used an ADVIA 2120i hematology system (Siemens, Berlin, Germany). After 48 hours of stimuli, cells were detached from the plates using TrypLE

Express and resuspended on 100 μL of PBS to be counted by cytometry.

Total RNA extraction, complementary DNA synthesis, and quantitative reverse transcription polymerase chain reaction analysis

Total RNA was purified using the Direct-zol RNA miniprep kit (Zymo Research, Irvine, CA) accordingly to manufacture´s instruction. Thereafter, 1 μg of total RNA was used as a template for reverse transcription using EpiScript Reverse transcription (Epicentre, Madison, WI) with random hexamer primers (Thermo Fisher Scientific). The complementary DNA (cDNA) obtained was subjected to qPCR performed on an ABI Prism 7500 detection system (Thermo Fisher Scientific) using Power SYBR Green PCR Master Mix (Thermo Fisher Scientific), as previously reported (32). The gene-specific primer sets are described in Supplemental Table 1. Relative changes in gene expression were calculated using the $2^{-\Delta\Delta Ct}$ normalized against the housekeeping gene *GAPDH*. For each pair of primers, a dissociation plot resulted in a single peak, indicating that only one cDNA species was amplified. Amplification efficiency for each pair of primers was calculated using standard curves generated by serial dilutions of cDNA obtained from unstimulated pSMCs (33).

Enzyme-linked immunosorbent assay

To quantify interleukin-6 and TNFα secretion, cells were grown for 24 to 72 hours in 1 mL of MCDB131 medium in one of the following conditions: 1 μg/mL LPS, 10^{-7} M LPS plus testosterone, or 10^{-7} M LPS plus testosterone-BSA or its vehicles. Media were collected, centrifuged at 4°C at 14,000 rpm for 15 minutes, and stored at −20°C. Cytokines were measured by commercially available sandwich enzyme-linked immunosorbent assay kits (BD Biosciences), according to the manufacturer's instructions.

Statistical analysis

All experiments were replicated at least three times with independent cell cultures. Data from three or more independent groups were analyzed using analysis of variance with Tukey as the posttest. Differences between two means were considered as statistically significance when $P < 0.05$. Statistical testing and calculation of western blot data were performed using the InfoStat (Faculty of Agricultural Sciences, National University of Córdoba, Córdoba, Argentina) statistical program.

Results

AR was localized at the plasma membrane of pSMCs

To determine the presence of the AR at the plasma membrane, we applied immunofluorescence staining to nonpermeabilized pSMCs. Positive staining was observed with a confocal laser microscope at the surface of intact cells [Fig. 1(a)]. Additionally, the colocalization of AR with the plasma membrane marker concanavalin A was detected and corroborated by Image J analysis, thus confirming its membrane localization [Fig. 1(a)]. To verify that the plasma membrane was impermeable to the antibody during the protocol, labeling for p65 was performed in the same conditions; as expected, no specific fluorescence was detected (not shown).

By western blot analysis, we determined AR was present in the purified plasma membrane fraction [Fig. 1(b)]; its localization at the cell surface was seen by immunofluorescence. Antibodies against p65 (part of the NF-κB complex) were used to control the absence of intracellular proteins in the membrane fraction [Fig. 1(b)].

We next determined the percentage of cells that expressed mAR. Flow cytometry showed a population (mean ± standard error) of 18.87% ± 2.43% of cells expressing mAR [Fig. 1(c)]. Accordingly, cell count for concanavalin A and AR by immunofluorescence yielded 17.88% ± 5.34% double-positive cells. Flow cytometry and immunostaining for p65 (exclusively intracellular expression) confirmed the integrity of the plasma membrane during the protocol [Fig. 1(c)].

mAR activation induced cell proliferation through mitogen-activated protein kinase signaling

Stimulation of pSMCs for a short time with testosterone or with the nonpermeable testosterone-BSA resulted in an increase in ERK1/2 phosphorylation [Fig. 2(a)]. The incubation with the inhibitor of protein palmitoylation 2-bromopalmitate prevented ERK phosphorylation after testosterone-BSA stimuli [Fig. 2(b)], demonstrating that palmitoylation is necessary for AR surface localization and membrane-initiated signaling in pSMCs. Additionally, testosterone and testosterone-BSA produced phosphorylation of Akt [Fig. 2(c)], indicating the activation of different signaling pathways by nongenomic androgen signaling.

Cell proliferation was evaluated by the nuclear expression of Ki67 and by total cell count. In line with previous reports (13), testosterone induced a substantial increase in cell proliferation. Interestingly, when the stimulation took place specifically through mAR by testosterone-BSA, a higher level of proliferation was observed as compared with testosterone-treated cells [Fig. 2(d)]. The AR inhibitor hydroxyflutamide and the ERK inhibitor U0126 prevented testosterone-BSA–stimulated proliferation [Fig. 2(d)], indicating the involvement of both AR and ERK signaling in this process. In agreement with the results obtained with Ki67 immunolabeling, membrane androgen stimuli significantly increased total cell number [Fig. 2(e)].

Because mAR stimulation resulted in higher pSMC proliferation, we wondered if intracellular AR activation might trigger both pro- and antiproliferative signals. The expression of the antiproliferative growth factor TGFβ1 was measured as a candidate for the differential effect of testosterone on cell proliferation. As shown in Fig. 2(f), only testosterone induced a substantial increase in

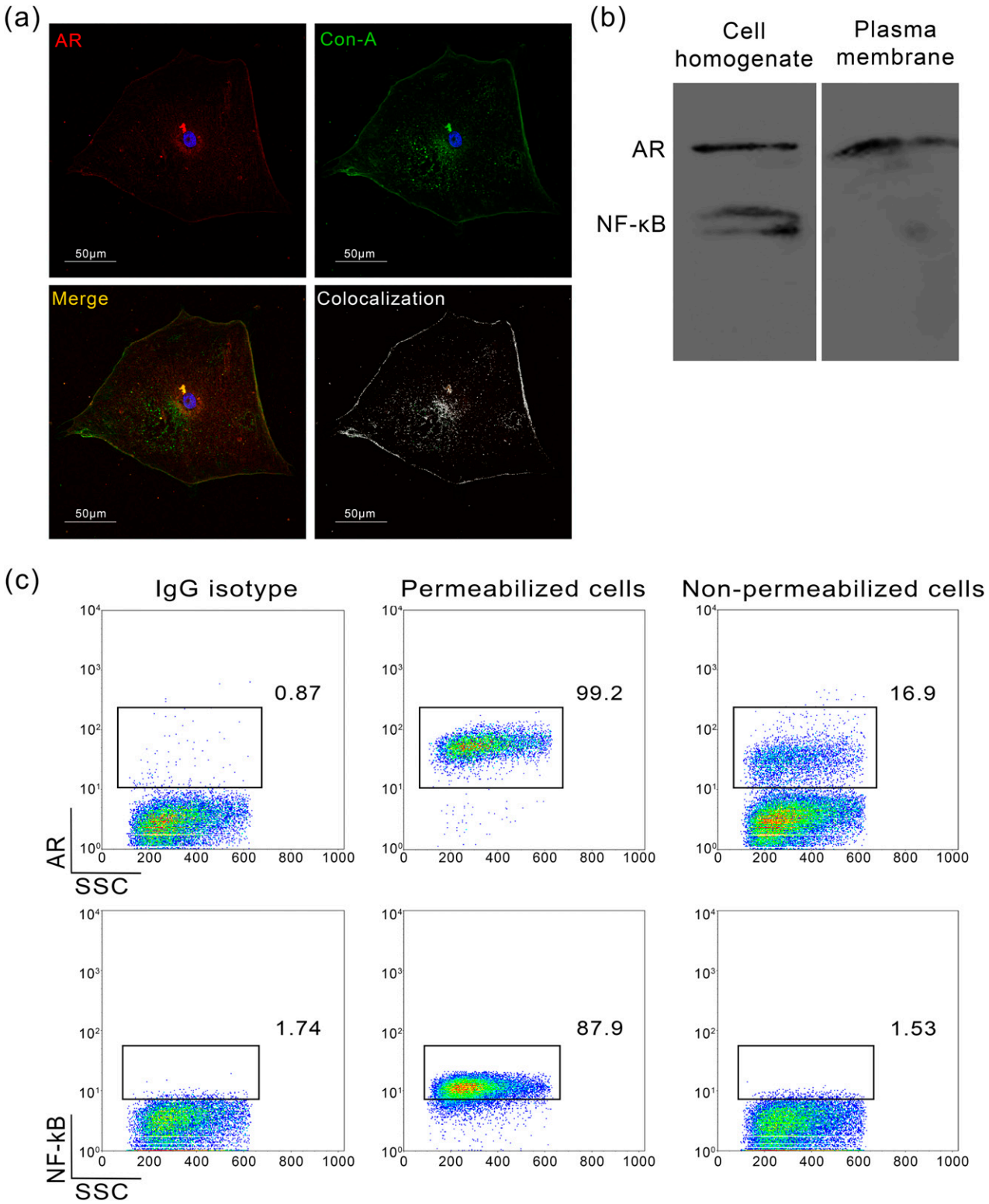

Figure 1. Localization of the AR at the cell surface of pSMCs. (a) pSMCs were analyzed by confocal laser microscopy using an antibody for AR (red), with specific staining displaying at the cell surface. Con-A was used as a membrane marker (green). By using the colocalization plugin from Image J, colocalization sites between AR and the cell membrane were determined (white pixels). (b) Concentrated biotin-isolated cell surface proteins from eight six-well plates were run on acrylamide gels. AR was detected on the cell surface fraction and on the whole-cell homogenate as a single band; the intracellular protein p65 was present in total homogenate but absent in the membrane fraction, discarding contamination with cytosolic proteins. (c) Permeabilized and nonpermeabilized pSMCs were analyzed by flow cytometry using anti-AR antibodies. This representative result of nonpermeabilized cells shows a population of 16.9% positive for surface AR. The average of three independent experiments indicated that the percentage of cells with surface AR is 18.87% ± 2.43%. Flow cytometry for NF-κB showed no positive staining in nonpermeabilized cells. Data are reported as mean ± standard error from three independent experiments. Con-A, concanavalin A–fluorescein isothiocyanate; IgG, immunoglobulin G; SSC, side scatter.

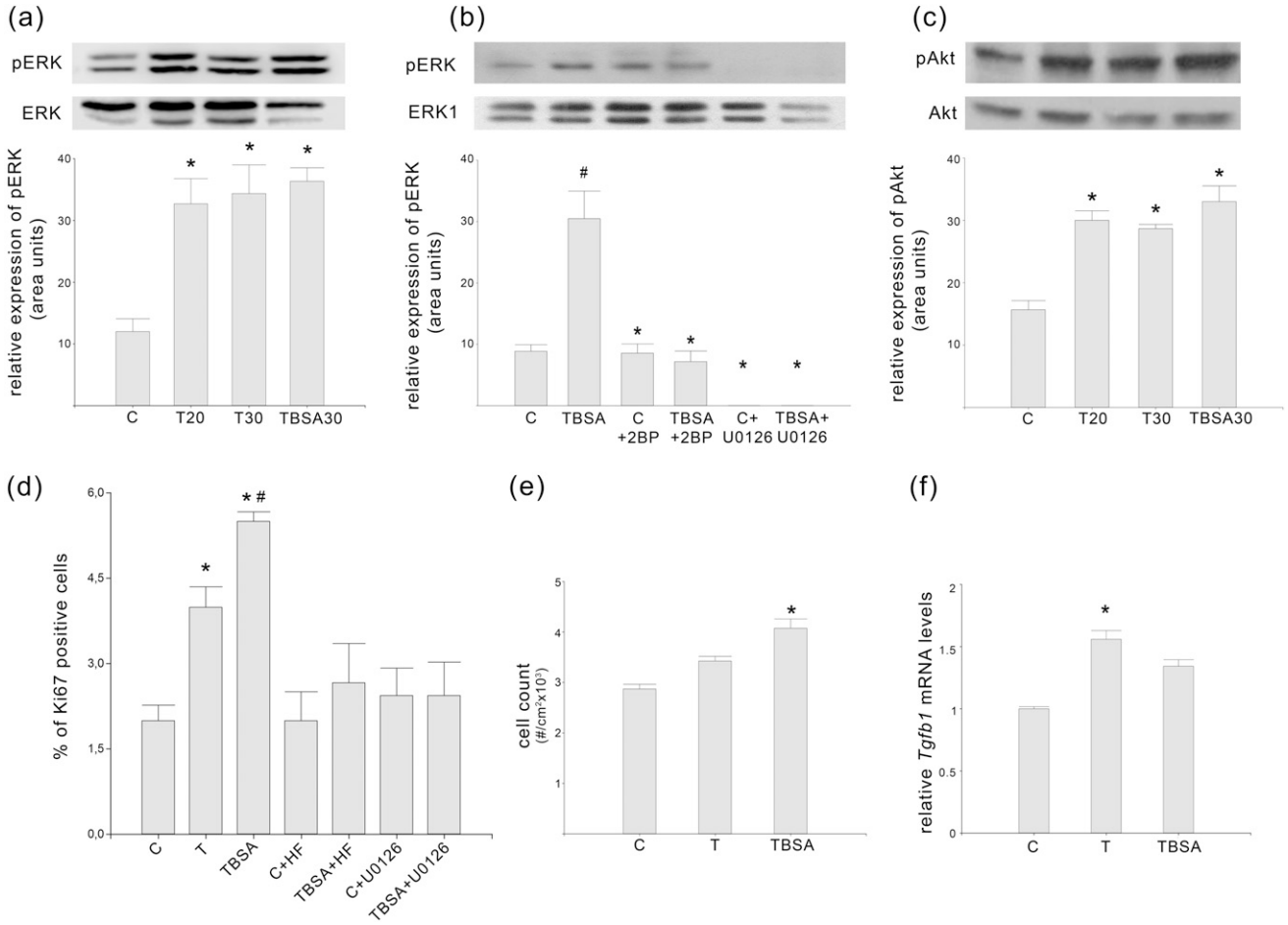

Figure 2. Testosterone signaling through mAR induced kinase phosphorylation, leading to cell proliferation. (a) pSMCs were stimulated for 20 or 30 minutes with testosterone, or for 30 minutes with TBSA or its control vehicles. A significant increase in ERK phosphorylation was observed in all treatments. $^{*}P < 0.05$ *vs* C. (b) Inhibitors of palmytoilation (*i.e.*, 2-bromopalmitate) and ERK phosphorylation (*i.e.*, U0126), applied 20 minutes before stimulation with TBSA, prevented ERK phosphorylation. $^{*}P < 0.05$ *vs* TBSA; $^{\#}P < 0.05$ *vs* C. (c) Total cell homogenates were also analyzed for Akt phosphorylation; a significant increase was observed after T20, T30, and TBSA stimulation. $^{*}P < 0.05$ *vs* C. (d) Immunocytochemistry for Ki67 was performed to determine cell proliferation after 24 hours of stimuli with testosterone or TBSA. The inhibitors for AR (*i.e.*, HF) and for ERK phosphorylation (*i.e.*, U0126) prevented TBSA-induced proliferation. $^{*}P < 0.05$ *vs* C; $^{\#}P < 0.05$ *vs* testosterone. (e) pSMCs were stimulated with testosterone or TBSA for 48 hours and the total number of cells was measured. Only TBSA stimulation induced a higher number of cells. $^{*}P < 0.05$ vs C. (f) pSMCs were stimulated for 6 hours for qPCR analysis, *Tgfb1* mRNA increased only after testosterone stimulation. $^{*}P < 0.05$ *vs* C. Data are reported as mean ± standard error from three independent experiments. Analysis of variance with Tukey posttest was used. C, control vehicle; HF, hydroxyflutamide; T, testosterone; T20, testosterone stimulation for 20 minutes; T30, testosterone stimulation for 30 minutes; TBSA, testosterone–bovine serum albumin; TBSA30, testosterone–bovine serum albumin stimulation for 30 minutes.

tgfβ1 mRNA. Our results indicate that membrane-initiated androgen signaling induced pSMC proliferation through mAR and ERK phosphorylation, whereas intracellular ARs increased TGFβ1 expression, which could be responsible for the modulation of cell proliferation (34).

It is well known that ARs need to bind AREs to regulate AR expression (35). Considering that pSMCs can respond to testosterone-BSA, we wondered if nongenomic membrane signaling could induce changes in AR expression. We observed a substantial increase in receptor expression only when cells had been stimulated with testosterone [Supplemental Fig. 1(a)]. qPCR analysis also indicated that testosterone must enter the cell to modify AR mRNA levels [Supplement Fig. 1(b)]. This result suggests that membrane-stimulated nongenomic androgen signaling does not participate in AR regulation.

Nongenomic androgen signaling favored the smooth muscle phenotype

Our group previously reported that androgens can modulate the pSMC phenotype (12, 13). Hence, we determined the participation of mARs in this process. We evaluated the expression of smooth muscle cell markers including α–smooth muscle actin and calponin, and the mesenchymal marker vimentin. A significant increase in mRNA levels for both smooth muscle markers and a decrease in vimentin mRNA expression were found 6 hours after stimulation with either testosterone or testosterone-BSA [Fig. 3(a)]. Protein expression of

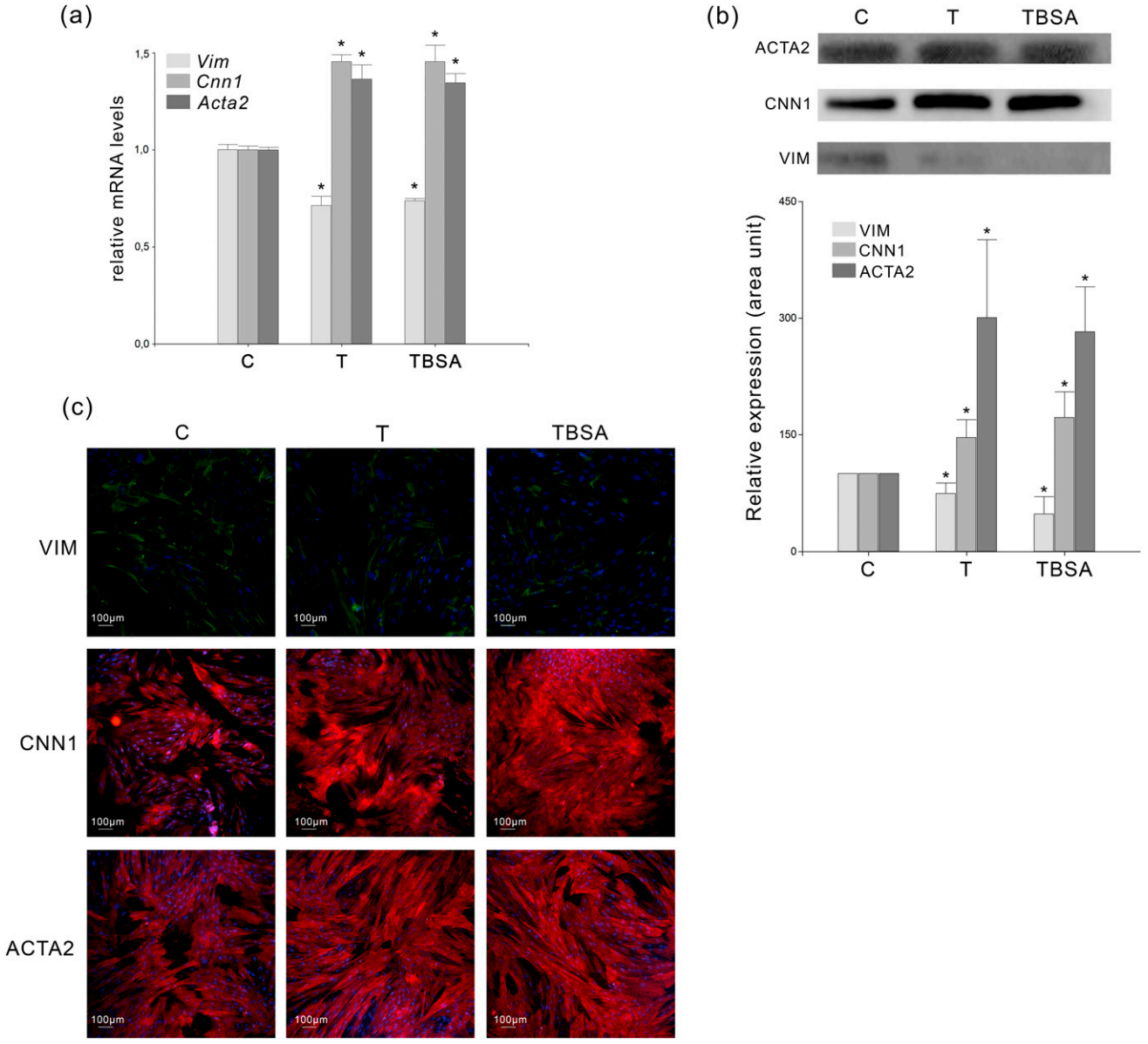

Figure 3. Nongenomic androgen signaling induced the smooth muscle phenotype. pSMCs were stimulated with testosterone, TBSA, or its control vehicle for (a) 6 hours for qPCR analysis, and (b) 24 hours for western blot or (c) immunofluorescence. (a) Testosterone and TBSA increased the expression of mRNA levels for the smooth muscle markers *Acta2* and *Cnn1* while decreasing mesenchymal marker *Vim* mRNA. $*P < 0.05$ *vs* C. (b, c) Protein expression determined by western blot and immunofluorescence also revealed an increase in CALP and ACTA2, and a decrease in VIM. $*P < 0.05$ *vs* C. Data are reported as mean ± standard error from three independent experiments. Analysis of variance with Tukey posttest was used. C, control vehicle; mRNA, messenger RNA; T, testosterone; TBSA, testosterone–bovine serum albumin.

phenotypic markers followed the same pattern as mRNA, as demonstrated by western blot [Fig. 3(b)] and immunocytochemistry [Fig. 3(c)]. These findings indicate that membrane-initiated androgen signaling on pSMCs favors the muscle phenotype.

Intracellular AR signaling was necessary for androgen modulation of pSMC response to LPS

pSMCs react against bacterial compounds such as LPS through the receptor TLR4. Once activated, TLR4-dependent signaling pathways induce nuclear translocation of NF-κB, secretion of proinflammatory cytokines, and cellular proliferation and dedifferentiation (4). Because testosterone has been reported to dampen this response (13), we addressed the involvement of mAR activation by costimulating pSMCs with LPS and testosterone-BSA. As expected, LPS induced the secretion of interleukin-6 and TNFα, whereas testosterone downregulated this response. By contrast, coincubation of LPS with testosterone-BSA had no effects on cytokine secretion compared with LPS alone, indicating that mAR signaling does not participate in this anti-inflammatory role of testosterone [Fig. 4(a) and 4(b)]. In line with results from our laboratory (13), LPS also induced a rapid

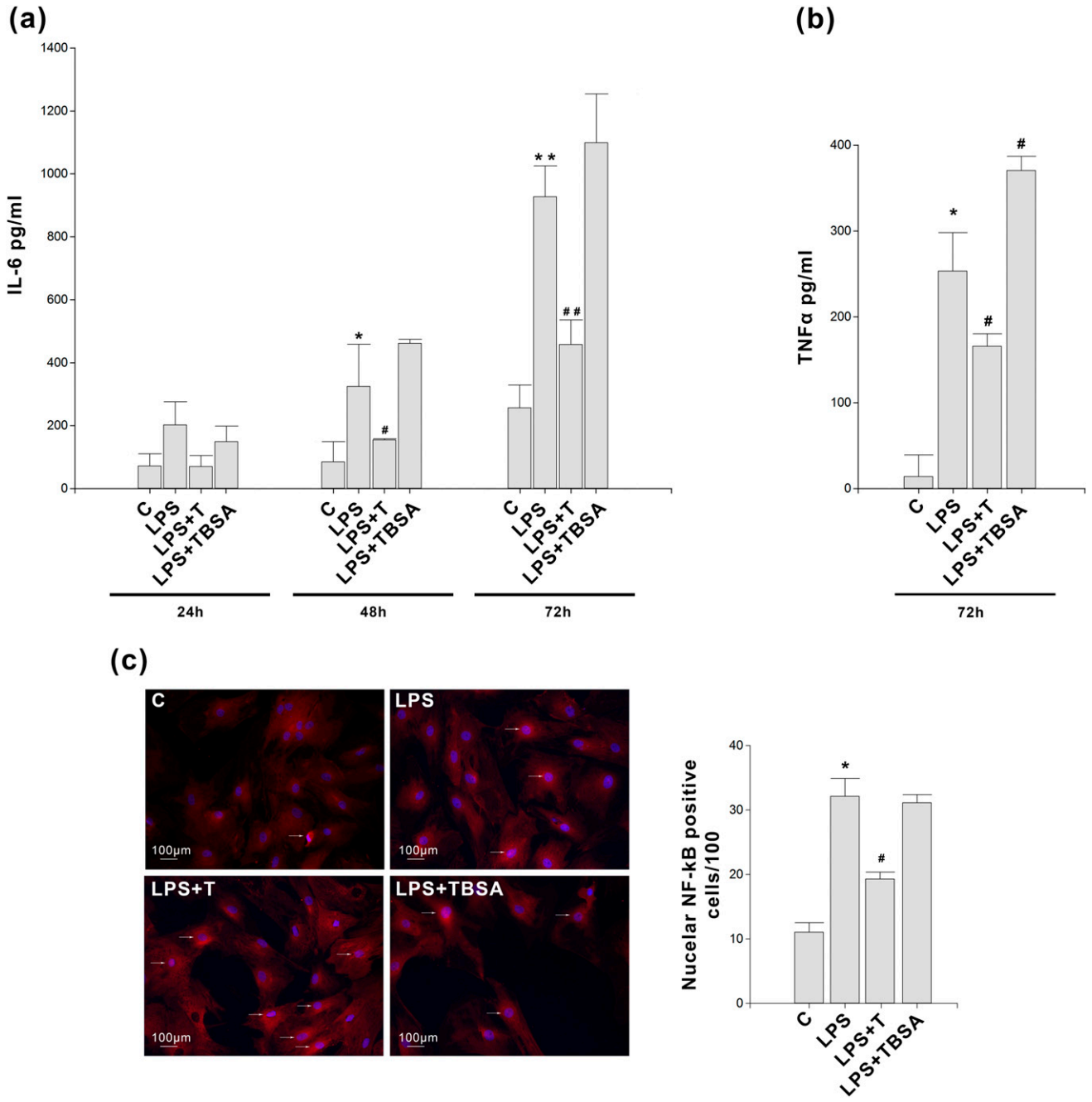

Figure 4. Modulation of inflammation by testosterone occurred through intracellular AR. pSMCs were stimulated with LPS, LPS+T, LPS+TBSA, or their control vehicles for 24 to 72 hours. (a, b) The secretion of IL-6 and TNFα was quantified by enzyme-linked immunosorbent assay in supernatants. The presence of testosterone inhibited the secretion of both proinflammatory cytokines, whereas TBSA did not alter the LPS-induced TNFα and IL-6 levels. (c) Immunofluorescence for p65 (red) was performed on pSMCs treated with LPS, LPS+T, or LPS+TBSA or their vehicles for 30 minutes. LPS stimulation induced NF-κB nuclear localization, which was modulated only by testosterone. Data are reported as mean ± standard error from at least three independent experiments. $^{*}P < 0.05$ *vs* control; $^{\#}P < 0.05$ *vs* LPS; $^{**}P < 0.01$ *vs* C; $^{\#\#}P < 0.01$ *vs* LPS (analysis of variance with Tukey posttest). C, control vehicle; LPS+T, lipopolysaccharide plus testosterone; LPS+TBSA, lipopolysaccharide plus testosterone–bovine serum albumin; T, testosterone; TBSA, testosterone–bovine serum albumin.

translocation of NF-κB to the nucleus, and its coincubation with testosterone downregulated this response. In contrast, the coincubation with testosterone-BSA did not significantly modify the number of NF-κB–positive nuclei induced by LPS [Fig. 4(c)]. These data indicate that the modulation of the inflammatory response by testosterone is due to cytosolic androgen signaling.

Consistently, testosterone downregulated LPS- and TNFα–induced mRNA expression of *TNF*, *IL6*, *IL1B*, *CCL2*, *CXCL5*, *IL1A*, *CXCL1*, and *IL19* in the LNCaP prostatic cell line, which expresses the classic intracellular AR, whereas testosterone-BSA did not exert effects on inflammatory-induced cytokine levels (Supplemental Fig. 2). To reinforce the concept of the need for intracellular

classic signaling for androgen anti-inflammatory actions, we used the PC3 prostatic cell line, which does not express intracellular AR. Stimulating PC3 with testosterone or testosterone-BSA resulted in a lack of modulation of LPS-induced cytokine expression (Supplemental Fig. 2).

Discussion

In the current study, we demonstrated that rat pSMCs expressed mARs capable of activating nongenomic-androgen signaling triggered by testosterone. In addition, we provide evidence for protein palmitoylation as one of the mechanisms involved in the translocation of the AR to the cell membrane, as well as for the activation of ERK and Akt as mediators of downstream noncanonical effects. Furthermore, proliferation and differentiation of pSMCs can be induced by signaling through receptors located at the plasma membrane, with mAR activation resulting in higher levels of cell proliferation than intracellular AR stimulation. On the other hand, modulation of AR expression and the immunoregulatory/anti-inflammatory effects of testosterone in pSMCs seem to be mediated mainly by stimulation of the cytosolic AR.

Evidence of nongenomic androgen signaling has been described in a variety of cells induced by receptors located at or near the plasma membrane, such as AR (17, 18), GPCR (19), SHBGR (36), and ZIP9 (20). Different studies have evaluated nongenomic effects on prostatic cells, including prostatic cancer epithelial cell lines LNCaP (37) and DU145 (23), as well as in primary cultured human stromal cells (24). LNCaP cells respond to a nonpermeable analog of testosterone by signaling through PI3K (21) and the Src-MEK-ERK-CREB pathway (27). Likewise, in primary cell cultures of uncharacterized human prostatic stromal cells, dihydrotestosterone induces ERK phosphorylation, enhances activity of the transcription factor Elk-1 (38), and can also induce EGFR-dependent calcium mobilization and MMP signaling (39). In comparison with these studies, our results focused on normal prostatic muscle cells, which are normally committed to homeostatic stromal-epithelial interactions (2). We demonstrate that, as for other stromal prostatic cells (24), pSMCs can respond to testosterone by a nongenomic mechanism inducing phosphorylation of ERK and Akt. In addition, the presence of AR at the cell surface of pSMCs was confirmed by different strategies, which is consistent with AR localization at the cell surface of LNCaP cells (22). The mechanism by which ARs migrate from the cytoplasm to the cell surface and bind to the plasma membrane is not fully understood. However, palmitoylation of amino acids in the E-domain of the AR has emerged as one of the mechanisms for surface localization and anchorage (25). Our data provide additional evidence about the participation of AR palmitoylation in pSMC membrane-initiated androgen signaling.

It is widely accepted that androgen signaling through the AR is crucial for prostate development and maintenance, because castration promotes a rapid and robust regression of the gland (8). At the cellular level, androgens stimulate epithelial cell proliferation, but little is known about the behavior of pSMCs under a microenvironment with androgen manipulation. This is striking considering that pSMCs play a central role in orchestrating prostate homeostasis in normal and in pathological conditions. We previously demonstrated that testosterone increases proliferation of pSMCs *in vitro* (13). Of note, nongenomic androgen stimulation initiated by mAR seems to be a stronger promoter of cell proliferation than classic AR. We hypothesize that testosterone may induce classic intracellular AR-mediated mechanisms that could partially compensate the highly proliferative effects incited by membrane receptors. In fact, cytosolic AR activation induced more TGFβ expression than mAR-initiated signaling. In normal conditions, a dynamic equilibrium would be generated between the effects of intracellular AR and those of the mAR, leading to homeostasis. Thus, changes in this equilibrium could tilt the balance from a homeostatic proliferation to a pathological state that could be crucial in the development and progression of BPH or prostate cancer.

Androgens promote pSMC differentiation by regulating the miodifferentiator complex Srf/Myocd (12). Moreover, stimulation with testosterone induced an increase of mRNA for muscle markers α–smooth muscle actin, calponin, and Lmod1 dose dependently (12), indicating that androgens maintain a differentiated state on pSMCs. The activation of mARs reproduces this response by stimulating nongenomic testosterone pathways. Although the mechanisms by which mARs control miodifferentiation are unknown, we propose a possible interaction between mAR signaling cascades and the SRF/Myocd pathway.

Inflammation of the prostate gland induces pSMC dedifferentiation *in vivo* (3, 4) and *in vitro* (3, 4). Testosterone counteracts LPS-induced dedifferentiation by favoring an anti-inflammatory response (13, 40). Results obtained in the current study indicate that LPS effects cannot be modulated through nongenomic signaling. Indeed, after costimulation of TLR4 (the LPS receptor) and mAR, pSMCs maintained the activation of NF-κB and the levels of proinflammatory cytokines induced by LPS. Cytosolic AR has been reported to suppress NF-κB directly (41), with this mechanism being likely responsible for the homeostatic anti-inflammatory effects of testosterone that are crucial for normal reproductive functions.

After the discovery of nongenomic androgen signaling, it became evident that testosterone could induce two independent cellular responses: activating ARE-regulated genes through cytosolic AR or ARE-independent genes regulated by other transcription factors when signaling through membrane receptors. These two pathways can also cross-talk in physiological conditions, leading to complex signaling mechanisms (42). Independent stimulation of nongenomic signaling has been related to different processes, including proliferation (28), apoptosis (20, 23), and cytoskeleton rearrangements (37) in a variety of cells. However, few reports elucidated differential outcomes of androgenic signaling through membrane *vs* cytosolic receptors. In this context, our results suggest that the final response executed by an androgen-targeted cell will be determined by the signaling activated by the AR.

In pSMCs, testosterone seems have some hyperproliferative, pathological effects induced by the mAR, whereas, through classic intracellular mechanisms, it could have a prohomeostatic role, including the inhibition of NF-κB signaling and the activation of antiproliferative molecules as TGFβ. Therefore, if these differential effects could be verified in human pSMCs, it would provide an important therapeutic target to block undesired effects of testosterone while preserving their homeostatic/anti-inflammatory actions. These findings will certainly encourage the development of new strategies through which the androgen signaling could be deliberately modified, and these findings pave the way for further research in the treatment of prostatic diseases.

Acknowledgments

Financial Support: This work was funded by Consejo Nacional de Investigaciones Científicas y Técnicas (CONICET PIP 2014-2016 No. 112 201301 00108 to C.A.M.), Secretaría de Ciencia y Tecnología Universidad Nacional de Córdoba (2014-2015 RR 1565/14 to C.A.M.), and Agencia Nacional de Promoción Científica y Tecnológica–Ministerio de Ciencia y Tecnología (PICT 2012-0654 to C.A.M.).

Correspondence: Amado Alfredo Quintar, MD, PhD, or Cristina Alicia Maldonado, PhD, Centro de Microscopia Electrónica, INICSA-CONICET, Facultad de Cs. Médicas, Universidad Nacional de Córdoba, Pabellón de Biología Celular, E. Barros esq. Enfermera Gordillo 1 piso Ciudad Universitaria, 5000 Córdoba, Argentina. E-mail: aquintar@cmefcm.uncor.edu or cmaldon@cmefcm.uncor.edu.

Disclosure Summary: The authors have nothing to disclose.

References

1. Flickinger CJ. The fine structure of the interstitial tissue of the rat prostate. *Am J Anat*. 1972;**134**(1):107–125.
2. Cunha GR. Mesenchymal-epithelial interactions: past, present, and future. *Differentiation*. 2008;**76**:578–586.
3. Quintar AA, Doll A, Leimgruber C, Palmeri CM, Roth FD, Maccioni M, Maldonado CA. Acute inflammation promotes early cellular stimulation of the epithelial and stromal compartments of the rat prostate. *Prostate*. 2010;**70**(11):1153–1165.
4. Leimgruber C, Quintar AA, Sosa LD, García LN, Figueredo M, Maldonado CA. Dedifferentiation of prostate smooth muscle cells in response to bacterial LPS. *Prostate*. 2011;**71**(10):1097–1107.
5. Lai KP, Huang CK, Fang LY, Izumi K, Lo CW, Wood R, Kindblom J, Yeh S, Chang C. Targeting stromal androgen receptor suppresses prolactin-driven benign prostatic hyperplasia (BPH). *Mol Endocrinol*. 2013;**27**(10):1617–1631.
6. Schauer IG, Rowley DR. The functional role of reactive stroma in benign prostatic hyperplasia. *Differentiation*. 2011;**82**:200–210.
7. Cunha GR, Hayward SW, Wang YZ. Role of stroma in carcinogenesis of the prostate. *Differentiation*. 2002; **70**:473–485.
8. Chang C, Lee SO, Wang RS, Yeh S, Chang TM. Androgen receptor (AR) physiological roles in male and female reproductive systems: lessons learned from AR-knockout mice lacking AR in selective cells. *Biol Reprod*. 2013;**89**(1):21.
9. Prins GS, Birch L, Greene GL. Androgen receptor localization in different cell types of the adult rat prostate. *Endocrinology*. 1991; **129**(6):3187–3199.
10. Antonioli E, Della-Colleta HH, Carvalho HF. Smooth muscle cell behavior in the ventral prostate of castrated rats. *J Androl*. 2004; **25**(1):50–56.
11. Hayward SW, Baskin LS, Haughney PC, Foster BA, Cunha AR, Dahiya R, Prins GS, Cunha GR. Stromal development in the ventral prostate, anterior prostate and seminal vesicle of the rat. *Acta Anat (Basel)*. 1996;**155**(2):94–103.
12. Leimgruber C, Quintar AA, Peinetti N, Scalerandi MV, Nicola JP, Miano JM, Maldonado CA. Testosterone rescues the dedifferentiation of smooth muscle cells through serum response factor/myocardin. *J Cell Physiol*. 2017;**232**(10):2806–2817.
13. Leimgruber C, Quintar AA, García LN, Petiti JP, De Paul AL, Maldonado CA. Testosterone abrogates TLR4 activation in prostate smooth muscle cells contributing to the preservation of a differentiated phenotype. *J Cell Physiol*. 2013;**228**(7):1551–1560.
14. Haynes JM, Frydenberg M, Majewski H. Testosterone- and phorbol ester-stimulated proliferation in human cultured prostatic stromal cells. *Cell Signal*. 2001;**13**(10):703–709.
15. Matsumoto T, Sakari M, Okada M, Yokoyama A, Takahashi S, Kouzmenko A, Kato S. The androgen receptor in health and disease. *Annu Rev Physiol*. 2013;**75**(1):201–224.
16. Levin ER. Rapid signaling by steroid receptors. *Am J Physiol Regul Integr Comp Physiol*. 2008;**295**(5):R1425–R1430.
17. Levin ER, Hammes SR. Nuclear receptors outside the nucleus: extranuclear signalling by steroid receptors. *Nat Rev Mol Cell Biol*. 2016;**17**(12):783–797.
18. Cheng J, Watkins SC, Walker WH. Testosterone activates mitogen-activated protein kinase via Src kinase and the epidermal growth factor receptor in sertoli cells. *Endocrinology*. 2007;**148**(5):2066–2074.
19. Pi M, Parrill AL, Quarles LD. GPRC6A mediates the non-genomic effects of steroids. *J Biol Chem*. 2010;**285**(51):39953–39964.
20. Thomas P, Pang Y, Dong J, Berg AH. Identification and characterization of membrane androgen receptors in the ZIP9 zinc transporter subfamily: II. Role of human ZIP9 in testosterone-induced prostate and breast cancer cell apoptosis. *Endocrinology*. 2014;**155**(11):4250–4265.
21. Papakonstanti EA, Kampa M, Castanas E, Stournaras C. A rapid, nongenomic, signaling pathway regulates the actin reorganization induced by activation of membrane testosterone receptors. *Mol Endocrinol*. 2003;**17**(5):870–881.
22. Lyng FM, Jones GR, Rommerts FF. Rapid androgen actions on calcium signaling in rat sertoli cells and two human prostatic cell lines: similar biphasic responses between 1 picomolar and 100 nanomolar concentrations. *Biol Reprod*. 2000;**63**(3):736–747.

23. Papadopoulou N, Charalampopoulos I, Anagnostopoulou V, Konstantinidis G, Föller M, Gravanis A, Alevizopoulos K, Lang F, Stournaras C. Membrane androgen receptor activation triggers down-regulation of PI-3K/Akt/NF-kappaB activity and induces apoptotic responses via Bad, FasL and caspase-3 in DU145 prostate cancer cells. *Mol Cancer*. 2008;**7**(1):88.
24. Peterziel H, Mink S, Schonert A, Becker M, Klocker H, Cato AC. Rapid signalling by androgen receptor in prostate cancer cells. *Oncogene*. 1999;**18**(46):6322–6329.
25. Pedram A, Razandi M, Sainson RC, Kim JK, Hughes CC, Levin ER. A conserved mechanism for steroid receptor translocation to the plasma membrane. *J Biol Chem*. 2007;**282**(31):22278–22288.
26. Migliaccio A, Castoria G, Di Domenico M, de Falco A, Bilancio A, Lombardi M, Barone MV, Ametrano D, Zannini MS, Abbondanza C, Auricchio F. Steroid-induced androgen receptor-oestradiol receptor beta-Src complex triggers prostate cancer cell proliferation. *EMBO J*. 2000;**19**(20):5406–5417.
27. Unni E, Sun S, Nan B, McPhaul MJ, Cheskis B, Mancini MA, Marcelli M. Changes in androgen receptor nongenotropic signaling correlate with transition of LNCaP cells to androgen independence. *Cancer Res*. 2004;**64**(19):7156–7168.
28. Sen A, O'Malley K, Wang Z, Raj GV, Defranco DB, Hammes SR. Paxillin regulates androgen- and epidermal growth factor-induced MAPK signaling and cell proliferation in prostate cancer cells. *J Biol Chem*. 2010;**285**(37):28787–28795.
29. Migliaccio A, Castoria G, Auricchio F. Analysis of androgen receptor rapid actions in cellular signaling pathways: receptor/Src association. *Methods Mol Biol*. 2011;**776**:361–370.
30. Fu R, Liu J, Fan J, Li R, Li D, Yin J, Cui S. Novel evidence that testosterone promotes cell proliferation and differentiation via G protein-coupled receptors in the rat L6 skeletal muscle myoblast cell line. *J Cell Physiol*. 2012;**227**(1):98–107.
31. Hatzoglou A, Kampa M, Kogia C, Charalampopoulos I, Theodoropoulos PA, Anezinis P, Dambaki C, Papakonstanti EA, Stathopoulos EN, Stournaras C, Gravanis A, Castanas E. Membrane androgen receptor activation induces apoptotic regression of human prostate cancer cells in vitro and in vivo. *J Clin Endocrinol Metab*. 2005;**90**(2):893–903.
32. Nicola JP, Peyret V, Nazar M, Romero JM, Lucero AM, Montesinos MM, Bocco JL, Pellizas CG, Masini-Repiso AM. S-Nitrosylation of NF-κB p65 Inhibits TSH-Induced Na(+)/I(-) Symporter Expression. *Endocrinology*. 2015;**156**(12):4741–4754.
33. Nazar M, Nicola JP, Vélez ML, Pellizas CG, Masini-Repiso AM. Thyroid peroxidase gene expression is induced by lipopolysaccharide involving nuclear factor (NF)-κB p65 subunit phosphorylation. *Endocrinology*. 2012;**153**(12):6114–6125.
34. Peehl DM, Sellers RG. Induction of smooth muscle cell phenotype in cultured human prostatic stromal cells. *Exp Cell Res*. 1997;**232**(2):208–215.
35. Grad JM, Dai JL, Wu S, Burnstein KL. Multiple androgen response elements and a Myc consensus site in the androgen receptor (AR) coding region are involved in androgen-mediated up-regulation of AR messenger RNA. *Mol Endocrinol*. 1999;**13**(11):1896–1911.
36. Heinlein CA, Chang C. The roles of androgen receptors and androgen-binding proteins in nongenomic androgen actions. *Mol Endocrinol*. 2002;**16**(10):2181–2187.
37. Kampa M, Papakonstanti EA, Hatzoglou A, Stathopoulos EN, Stournaras C, Castanas E. The human prostate cancer cell line LNCaP bears functional membrane testosterone receptors that increase PSA secretion and modify actin cytoskeleton. *FASEB J*. 2002;**16**(11):1429–1431.
38. Cato AC, Nestl A, Mink S. Rapid actions of steroid receptors in cellular signaling pathways. *Science's STKE* 2002;**2002**:re9.
39. Oliver VL, Poulios K, Ventura S, Haynes JM. A novel androgen signalling pathway uses dihydrotestosterone, but not testosterone, to activate the EGF receptor signalling cascade in prostate stromal cells. *Br J Pharmacol*. 2013;**170**(3):592–601.
40. Quintar AALC, Leimgruber C, Pessah OA, Doll A, Maldonado CA. Androgen depletion augments antibacterial prostate host defences in rats. *Int J Androl*. 2012;**35**(6):845–859.
41. Nelius T, Filleur S, Yemelyanov A, Budunova I, Shroff E, Mirochnik Y, Aurora A, Veliceasa D, Xiao W, Wang Z, Volpert OV. Androgen receptor targets NFkappaB and TSP1 to suppress prostate tumor growth in vivo. *Int J Cancer*. 2007;**121**(5):999–1008.
42. Hammes SR, Davis PJ. Overlapping nongenomic and genomic actions of thyroid hormone and steroids. *Best Pract Res Clin Endocrinol Metab*. 2015;**29**(4):581–593.